STABILITY ANALYSIS ON NATURAL LAMINAR FLOW WING IN SUPERSONIC FLOW: ONERA-JAXA JOINT RESEARCH PROGRAM

Kenji YOSHIDA*, Yoshine UEDA*, Daniel ARNAL, Jean-Pierre ARCHAMBAUD****
***JAXA(Japan Aerospace Exploration Agency),**
****ONERA(The French Aerospace Laboratory)**
yoshida.kenji@jaxa.jp; daniel.arnal@onera.fr

Keywords: *Supersonic, Natural laminar flow wing, Transition analysis, Flight test*

Abstract

Stability analysis on the supersonic natural laminar flow (NLF) wing designed by JAXA in flight test condition was performed as a joint research program between ONERA and JAXA. Both parties validated the NLF wing effect by confirming suppression of crossflow instability at design point, using an e^N method with fixed β strategy proposed by ONERA. Although JAXA's flight test vehicle had averaged roughness height of about 1 μm, our roughness study based on ONERA's database showed there was little influence on measured transition location. Furthermore, it was found that measured pressure distribution did not completely coincide to the target pressure distribution (Cp_{Target}) for the NLF wing design. It revealed forward transition location at outer wing region in flight test, compared with the transition location predicted with the Cp_{Target} which had large gain to delay the transition. Reynolds number influence on transition location has been studied using the Cp_{Target}: transition location, $(x/c)_{Tr.}$, rapidly moves from mid-chord location to forward location (near leading edge) at a certain Reynolds number condition, according to change of instability mode from Tollmien-Schlichting instability to crossflow instability.

1 Introduction

Skin friction drag reduction due to natural laminar flow (NLF) wing is one of key design concepts for a future supersonic transport. Firstly, Japan Aerospace Exploration Agency (JAXA) created an NLF wing design concept and confirmed transition delay in flight test with an experimental vehicle called "NEXST-1" in the National EXperiment Supersonic Transport (NEXST) program. To understand the NLF wing design concept in detail, stability analysis in laminar boundary layer was undertaken. Before the flight test, using analysis tools [1], JAXA and ONERA started a joint research on the stability analysis and transition prediction in the framework of NEXST program. After the flight test, both parties focused on making clear physical mechanism leading to laminar to turbulent transition on the NLF wing by comparing stability analysis and experimental results.

This paper provides recent principal results of stability analysis on the NLF wing in our joint research program. In Section 2, summary of the NLF wing design and flight test results are introduced as background. Then, outline of analysis approach to investigate stability characteristics of the boundary layer developing on the NLF wing as well as flight test principal results are described in Section 3. Finally, Reynolds number effect and influence of surface roughness are discussed in Section 4.

2 Summary of NEXST-1 NLF Wing Design

2.1 Design Concept

To realize NLF condition on a highly swept wing, it is very important to control crossflow instability. JAXA found an ideal pressure distribution to suppress it by using a current

transition analysis method (e^N method) and developed a CFD-based inverse design method to realize it on supersonic transport (SST) configurations [2]. The design procedure of present method is illustrated in Fig. 1. The most important part in this procedure is to specify a target pressure coefficient distribution (Cp_{Target}) which consists of an ideal pressure distribution on upper surface and the difference of Cp distributions on upper and lower surfaces satisfied with "warped" wing design condition.

According to the procedure, JAXA firstly prepared an initial configuration designed with some pressure drag reduction concepts based on supersonic linear theory, that is an arrow planform, a warped wing and an area-ruled body. Then, the difference between the Cp_{Target} and CFD calculated Cp distribution on the initial configuration was estimated. After that, the configuration was modified to reduce the difference of Cp distributions by using supersonic lifting surface theory. Finally, such a step was continued to reduce the difference.

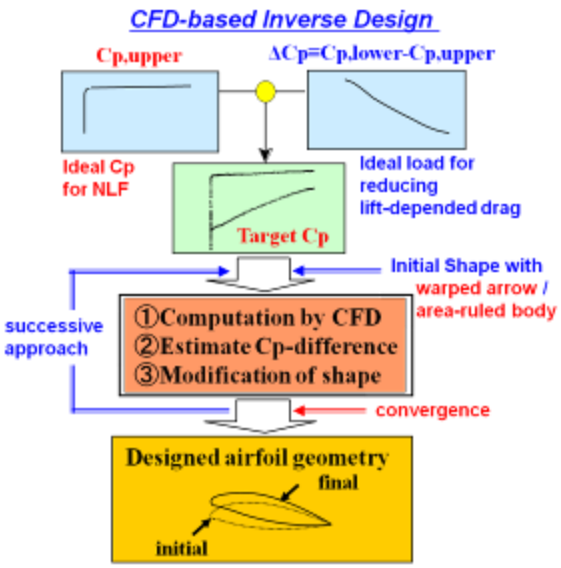

Fig. 1. CFD-based inverse method for NLF wing design

To demonstrate the NLF wing design concept in flight test, JAXA designed and developed an unmanned and scaled supersonic experimental vehicle (NEXST-1) shown in Fig. 2, which was manufactured taking account of elastic deformation at the design point (Mach number M=2.0, lift coefficient C_L=0.1 and flight altitude H=18km). It also includes four design concepts to reduce supersonic airframe drag. The design process and principal results are described in Ref. [2] in detail.

Fig. 2. NEXST-1 with aerodynamic design concepts

2.2 Flight Test and Wind Tunnel Test Validations

Before the flight test, JAXA experimentally confirmed the NLF wing design concept using a special wing-body wind tunnel model which consisted of adiabatic material skin (about 5 mm thickness on metal body) and multi-element type hot-films. The continuous supersonic wind tunnel of ONERA (S2MA) was chosen to investigate transition characteristics since its turbulence level Tu was firstly considered as rather low: 0.15%<Tu<0.20%. Nonetheless, these values remain high compared to very weak turbulence level in free flight condition: Tu<0.05%: therefore, the NLF wing design was qualitatively confirmed but not quantitatively in terms of transition location [3]. Furthermore, the stability analysis on the wind tunnel test conditions was also conducted, and recent results were summarized in Ref. [4].

Then, the flight test was conducted at the Woomera test field in Australia in 2005. The test consisted of two aerodynamic measurement phases. One was "angle of attack (AOA) sweep test" phase around 18km altitude to confirm the drag characteristics of the NEXST-1. Another was "altitude sweep test" phase while maintaining C_L at the design value of 0.1 to investigate the effect of NLF wing concept at higher Reynolds number conditions than at the design point.

To realize the NLF wing concept in real flight vehicle, severe criterion for surface smoothness condition was specified. To detect transition characteristics, hot-film sensors, dynamic pressure transducers, Preston tubes, and thermocouples were applied, then the correlation among their signals was confirmed in a wind tunnel test before the flight test [5].

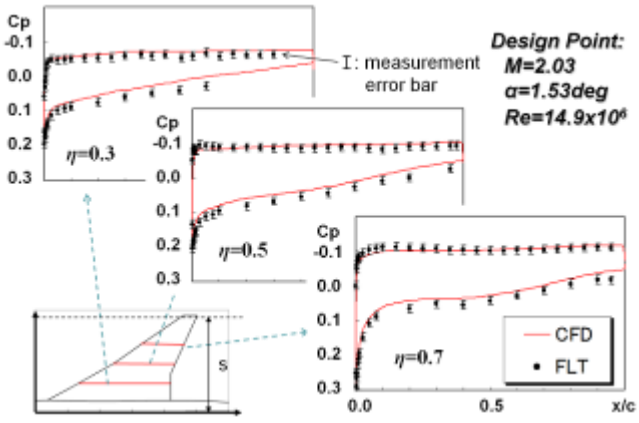

(a) Pressure distributions at design point [5]

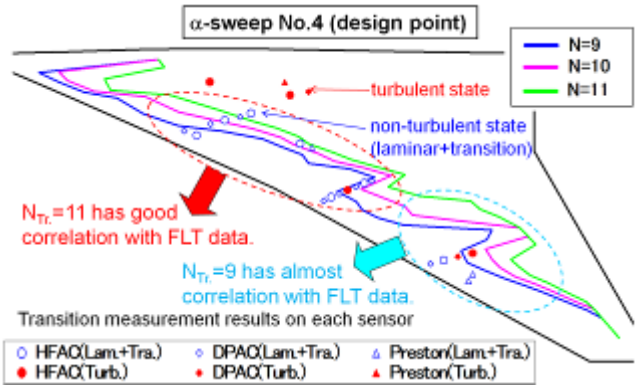

(b) Transition data in previous joint research [1]

Fig. 3. Principal results in flight test

One of principal results of the flight test is summarized in Fig. 3(a). This figure shows a comparison between measured and CFD-based Cp distributions on the wing at the design condition ("α_No.4"). These computations were performed on elastic deformed configuration [5]. Especially, high correlation between them on upper surface was confirmed within measurement error bar of $\Delta Cp=\pm 0.0115$ illustrated as symbol of "I" in Fig. 3(a). It indicates that necessary conditions to obtain extended laminar regions on the wing were satisfied during the flight test.

Fig. 3(b) shows comparison of measured transition pattern and JAXA's transition analysis results [1, 5]. Solid-red and open-blue symbols correspond to turbulent and non-turbulent state in boundary layer at the design point. Here non-turbulent means laminar and transition states. Measured transition data indicate approximately 40% laminarity on upper surface. Three solid-lines correspond to transition lines predicted with assumed transition criteria for N contours based on a current e^N method. JAXA improved an in-house e^N code under the framework of ONERA-JAXA joint research program [1] and used so-called envelope strategy [6] to compute amplification rate in stability analysis. In this comparison, transition location at inner wing region predicted with N=11 seems to be in good agreement with measured data, whereas a lower value N=9 matches with measured transition pattern in the outer wing region [1]. This non-unique transitional N factor value, contrary to what was expected, highlights the fact that distinct transition mechanisms may exist in inner and outer part of the wing. This is strong motivation to advance present ONERA-JAXA joint research activity.

3 Stability Analysis in Flight Test Conditions

3.1 Analysis Approach

To reduce discrepancy between measured and predicted transition pattern at the design condition shown in Fig. 3(b), the following subjects were investigated; (i) to check the Cp distribution to be used for computing laminar boundary layer (LBL), (ii) to understand physical mechanism, indentifying the most dominant mode (Tollmien-Schlichiting instability or crossflow instability), (iii) to consider influence of surface roughness, and (iv) to obtain Reynolds number effect on transition characteristics. Outline of our approach to them is as follows:

(1) Improving Cp distributions [Subject (i)]

Although CFD-based Cp distributions are definitely located within measurement error bar of measured pressure coefficients as shown in Fig. 3(a), there is slight difference between them. It might have possibility to affect growth of LBL. Therefore, JAXA improved the Cp distribution used to compute boundary layer by applying a surface-interpolation technique on the difference between measured and computed pressure coefficients. It consists of a combination of least square approximation technique for chordwise direction and constrained spline function fitting technique for spanwise direction. Fig. 4(a) shows a comparison of present surface-interpolated Cp contour which will be used to conduct stability analysis and initial CFD-based Cp contour.

In present stability analysis, JAXA selected the following three cases; (A) at design point case called "α_No.4", (B) at off-design point case called "α_No.2", and (C) at higher Reynolds number case called "Re_No.5". Their detail conditions are described in Fig.9, 11 and 14. Concerning the case Re_No.5, interpolated Cp distribution was used as input for boundary layer computation. For the off-design point, case α_No.2, CFD-based pressure distribution was considered because it was very little different from measured one. Fig. 4(b) shows comparison of some Cp distributions along chordwise location at inner and outer wing regions at y/s=0.3 and 0.7 where s stands for the semi-span of the model s=2.36 [m].

(2) Fixed β strategy [Subject (ii)]

It is important to split crossflow instability (CFI) mode and Tollmien-Schlichting instability (TSI) mode on the NLF wing to understand physical nature of transition on three-dimensional boundary layer. In our previous analysis [1], both parties used envelope strategy which was one of models to reduce computational cost by neglecting freedom of physical variables in three dimensional disturbances. In the framework of classical linear stability theory, disturbances are introduced as:

$$q'(x,y,z,t) = \hat{q}(z)\cdot\exp(-\alpha_i x)\cdot\exp\left(i(\alpha_r x + \beta y - \omega t)\right)$$

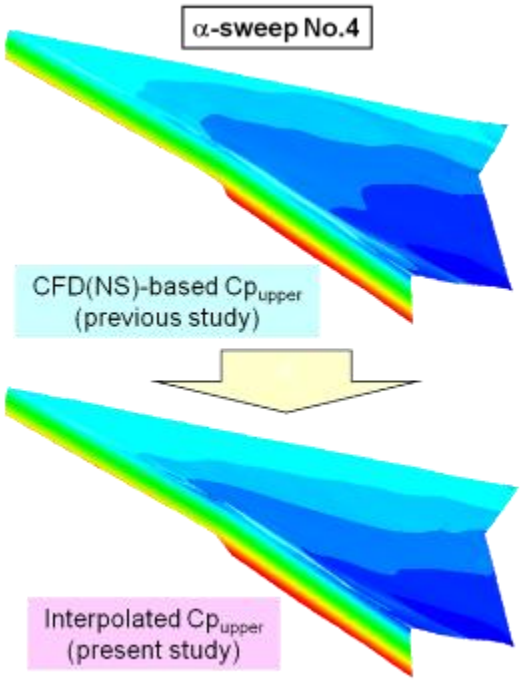

(a) Previous and present Cp contours at the design point

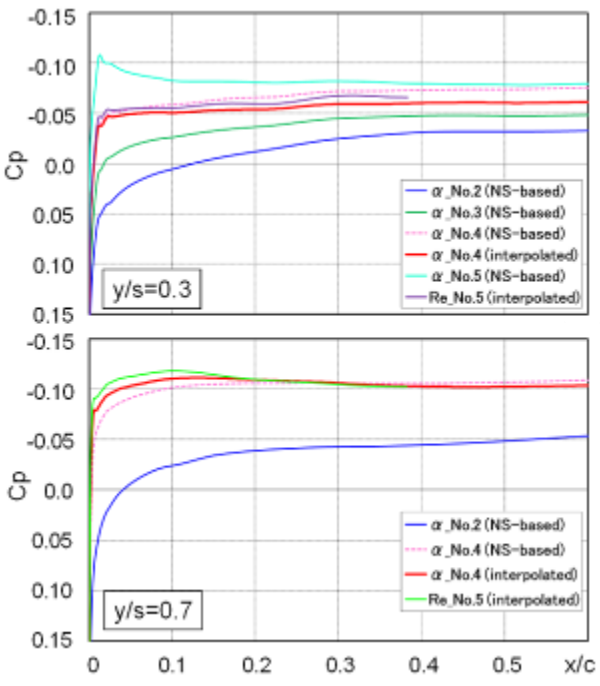

(b) Chordwise Cp distributions in present study

Fig. 4. Pressure distributions for laminar boundary layer

where q' is a fluctuation (velocity, pressure or temperature) and $\hat{q}$ its amplitude function (here $\boldsymbol{x}$ is perpendicular to the leading edge and $\boldsymbol{z}$ normal to the wall) as represented in Fig. 5. Considering the spatial theory, $\alpha=\alpha_r+i\alpha_i$ is the complex wavenumber in the $\boldsymbol{x}$ direction. The

spanwise wave-number β (***y*** direction parallel to the leading edge) and frequency ω are real. It is common to introduce the angle between the external streamline and the wave number vector

$$\psi = \tan^{-1}(\beta/\alpha_r) - \theta_0$$

where θ_0 represents the angle between the external streamline and the vector **x** (see Fig. 5).

Envelope strategy consists of selecting a special propagation direction (ψ_m) which has maximum amplification rate ($\sigma \equiv -\alpha_i$) among whole propagation direction angles ($-90^\circ \le \psi \le 90^\circ$) at each frequency ($f$[Hz]) and streamwise Reynolds number based on chordwise location (Re_x). This model can not explicitly split CFI and TSI modes, because selection of ψ_m always means to indicate maximum value on σ of CFI or TSI modes.

An improvement of this approach lies in the so-called fixed β strategy [6]. In this strategy, several pre-set combinations of (β_r, f) are applied to compute eigenvalues (α_r, α_i) in linear stability equation in spite of selecting ψ_m. ONERA has reported its effectiveness on several transition studies in both low and transonic speeds [7]. The application of such fixed β strategy to our NLF wing in supersonic flow is one of valuable challenges for ONERA as well as JAXA.

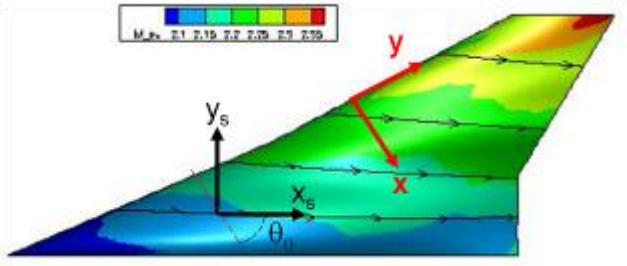

Fig. 5. Mach number color map and freestream lines for case α_No.4. Definition of the wing system axes (x,y,z) and external streamline ones (x_s,y_s,z).

(3) Rk study [Subject (iii)]

The NEXST-1 airplane was carefully manufactured and polished to keep severe surface roughness condition for little influence on transition phenomenon. Before and after the flight test, surface roughness data on the NEXST-1 were measured with a special technique illustrated in Fig. 15. According to the ONERA's database on relation between averaged roughness height (k) and transition N value [7], JAXA estimated so-called Rk value which was defined as Reynolds number on averaged roughness height, and investigated influence of roughness on transition measurement data. The main results are mentioned in Section 4.

(4) Stability analysis at higher Reynolds number conditions [Subject (iv)]

Reynolds number effect on transition phenomenon on the NLF wing is the most important subject to establish the NEXST-1 aerodynamic design technology. In the flight test, transition characteristics at higher Reynolds number condition $\mathrm{Re}_{MAC}=32.5\times10^6$ (case Re_No.5), which was about 2.5 times of Reynolds number at the design point $\mathrm{Re}_{MAC}=13.4\times10^6$ (case α_No.4), were measured. (Here, Re_{MAC} is Reynolds number based on mean aerodynamic chord.) Then, stability analysis was also performed and compared with transition measurement data. Furthermore, transition characteristics on the Cp_{Target} were carefully investigated by applying fixed β strategy. The principal results are summarized in Section 4.

3.2 Stability Analysis At Design Point

To improve the discrepancy between measured and transition analysis results as shown in Fig. 3(b), ONERA and JAXA directly applied present surface-interpolated Cp distribution to compute LBL characteristics, in place of using CFD(NS)-based LBL results in previous study. As a typical LBL result, crossflow velocity profiles plotted in external streamline coordinates (normalized with resultant velocity Ue at edge of LBL) are summarized in Fig. 6. In Fig. 6, "z" is the wall normal direction.

Then, both parties computed N factors with envelope strategy and compared them as shown in Fig. 7. This figure also includes measured transition location (as indicated by "$X_T$exp") and special N values due to these locations (called "transition N value: $N_{TR.}$").

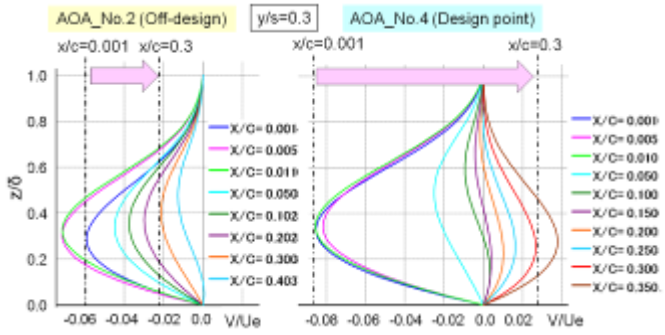

(a) y/s=0.3 (inner wing region)

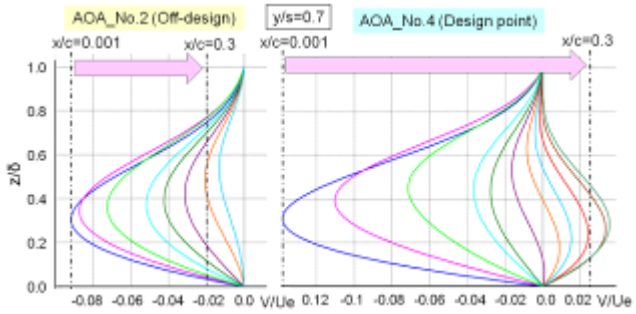

(b) y/s=0.7 (outer wing region)

Fig. 6. Crossflow velocity growth at design point and off-design point. Velocity profiles are plotted in external streamline coordinates. (Here, x means x_s.)

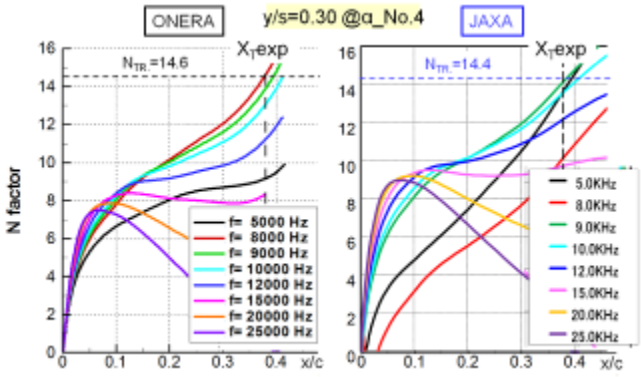

(a) y/s=0.3 (inner wing region)

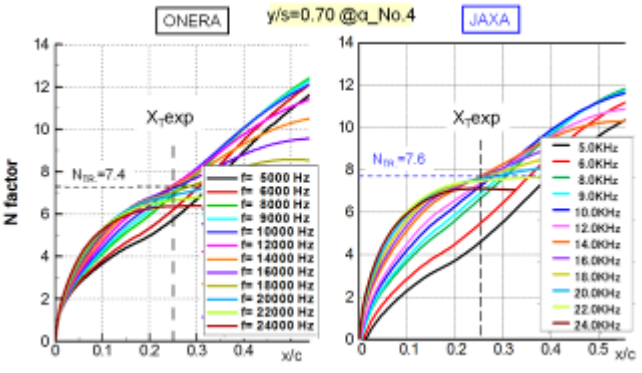

(b) y/s=0.7 (outer wing region)

Fig. 7. Stability characteristics with envelope strategy at design point

As similar to previous study, JAXA's N factors and $N_{TR.}$ are in good agreement with ONERA's results. Against our expectation, the $N_{TR.}$ at inner wing region is about two times higher than that at outer region. If it is assumed that the $N_{TR.}$ should be constant over whole spanwise stations, JAXA thinks that the measured transition location at outer region is forced to be located more forward than the location predicted with the constant $N_{TR.}$. This is discussed at Section 4 again.

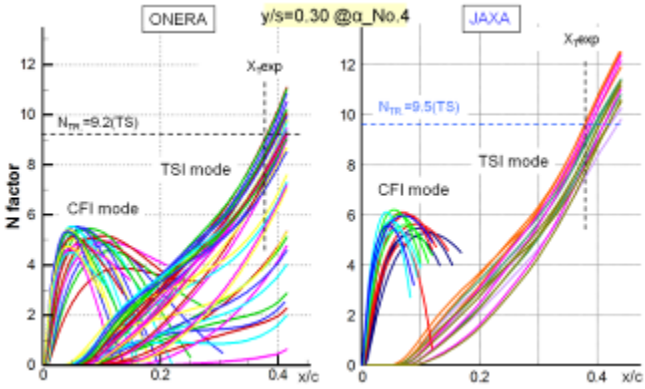

(a) y/s=0.3 (inner wing region)

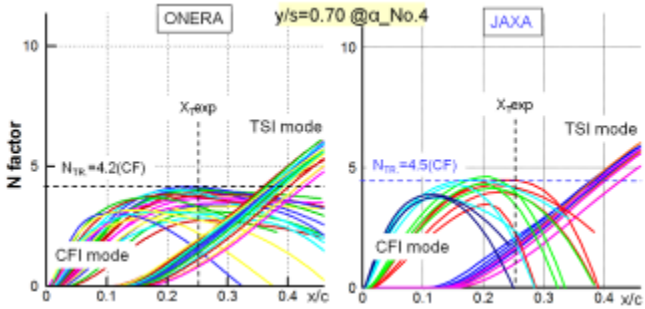

(b) y/s=0.7 (outer wing region)

Fig. 8. Stability characteristics with fixed β strategy at design point

Fig. 8 shows similar comparison of N factors computed by both parties with fixed β strategy. The range of several combinations of (β_r , f) was specified as follows:

$$-450 \le \beta_r[m^{-1}] \le 3000 \quad , \quad 3 \le f[kHz] \le 25$$

These were based on present stability analysis results with envelope strategy. As easily seen in the figure, contrary to envelope method, fixed β strategy can clearly split instabilities into two modes: crossflow instabilities (CFI) on one hand and Tollmien-Schlichting instabilities (TSI) on the other hand. N factors due to CFI

mode (N_{CFI}) rapidly increase near the leading edge where the flow is accelerated (high negative pressure gradient) as illustrated in Fig. 4(b), then N factors due to TSI mode (N_{TSI}) gradually grows after the maximum of the N_{CFI} in region where the pressure gradient is weakly negative or positive (see Fig. 4(b)). According to the measured transition data, it is recognized that the most dominant mode is TSI in inner wing region (y/s=0.3), whereas CFI dominates transition process in the outer region (y/s=0.7) as shown in Fig. 8(b).

Further stability analysis at other spanwise stations with fixed β strategy revealed the most dominant instability mode over the whole wing region as shown in Fig. 9. This figure also includes predicted transition lines based on some typical N values provided by envelope strategy. Comparing the figure with Fig. 3(b), a slight improvement was obtained at inner wing region using present surface-interpolated Cp distribution. But certain discrepancy between measured and predicted transition location still exists.

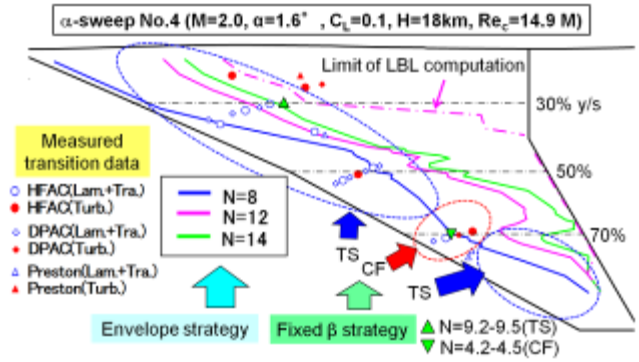

Fig. 9. Comparison of transition analysis and measurement results at design point

From the figure, it was confirmed that, except in a narrow zone around y/s≈0.7, CFI was suppressed very well, namely the most dominant mode responsible for transition onset was TSI. This origin exists in the fact that the transition at outer region (y/s=0.7) was measured relatively forward as explained previously. There might be a few possibilities, for example, influence of surface roughness on transition phenomenon, small spanwise deviation between measured and target Cp contours, and so on. Before discussing them, to understand effectiveness of present Cp distribution on suppressing CFI clearly, influence of angle of attack (AOA), on transition process has been studied and summarized in next sub-section.

3.2 Stability Analysis At Off-Design Point (Other AOA Condition)

In the flight test, 6 steps of AOA were specified and the design point was realized at the 4th step (α_No.4). As typical off-design point condition, the 2nd step (α_No.2), such as AOA=-0.09° corresponding to a lift coefficient of C_L=0.04, was chosen. Figs. 10(a) and (b) show N factors computed with envelope and fixed β strategies, respectively. The range of several combinations of (β_r, f) was specified as follows:

$$-500 \le \beta_r[m^{-1}] \le 3000 \quad , \quad 3 \le f[kHz] \le 20$$

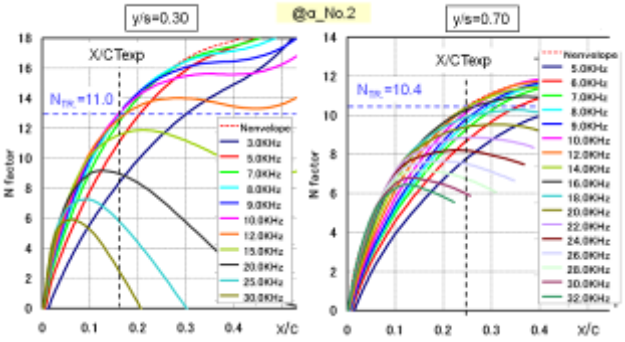

(a) Envelope strategy

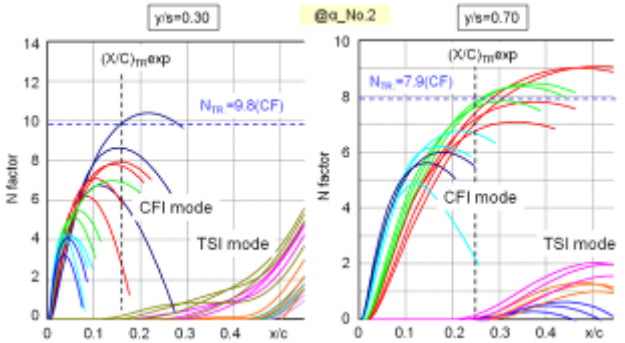

(b) Fixed β strategy

Fig. 10. Stability characteristics at α_No.2 (off-design point)

As easily seen in Fig. 10(a) and (b), N factors at present AOA case are larger than them at the design point (shown in Fig. 7 and 8). By comparing N factors and measured transition

location, it is clear that the CFI mode is the dominating one and responsible for an early transition. Naturally, this originates in the Cp distributions illustrated in Fig. 4 and crossflow velocity profiles shown in Fig. 6. Main reason of non-suppression of CFI mode at α_No.2 lies in the evolution of crossflow velocity profile in the boundary layer. For the off-design configuration, the crossflow velocity component (plotted in streamline coordinates) in the boundary layer thickness remains negative moving downstream as represented in Fig. 6: this means that the crossflow velocity is orientated towards the concavity of the external streamline. On the other hand, at the design point, the crossflow velocity is still negative in the leading edge region but rapidly changes its sign and keep weak values reducing the amplification of CFI. Therefore, the NLF wing design concept is based on suppression of CFI due to existence of reverse change of crossflow direction.

Fig. 11 shows comparison of measured transition data and N factors computed with both envelope and fixed β strategies at several spanwise stations. N=10 provided by envelope strategy is in good agreement with measured transition location. Stability analysis obtained with fixed β strategy reveals that the CFI mode is dominant on transition phenomenon except for tip region (y/s=0.9). This means that the shape of Cp distribution at the design point, which is almost the same as the Cp_{Target}, is the only effective one to suppress CFI mode. On the other hand, other shape of Cp distribution, especially near leading edge at off-design point has no potential to suppress CFI. It becomes one of evidences for validation of JAXA's NLF wing design concept.

3.3 Stability Analysis At Higher Reynolds Number Condition

Stability analysis with both envelope and fixed β strategies was performed at Re_No.5. Figs. 12(a) and (b) show comparison of stability analysis results with envelope strategy computed by ONERA and JAXA. There is almost agreement between them, but transition N value is slightly different. At higher Reynolds number condition, to solve eigenvalue problem is more sensitive on numerical errors than at lower Reynolds number condition.

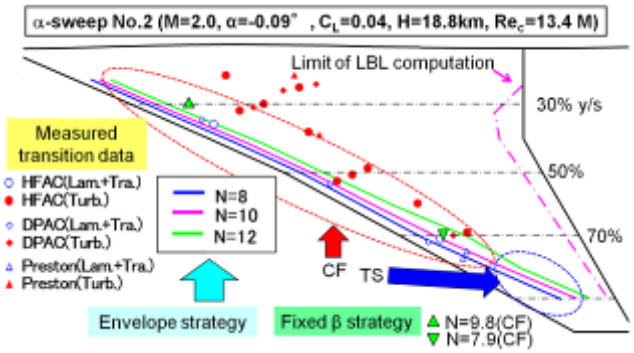

Fig. 11. Comparison of transition analysis and measurement results at off-design point

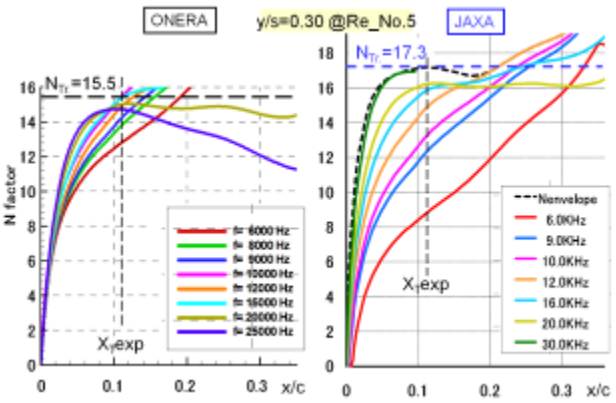

(a) y/s=0.3 (inner wing region)

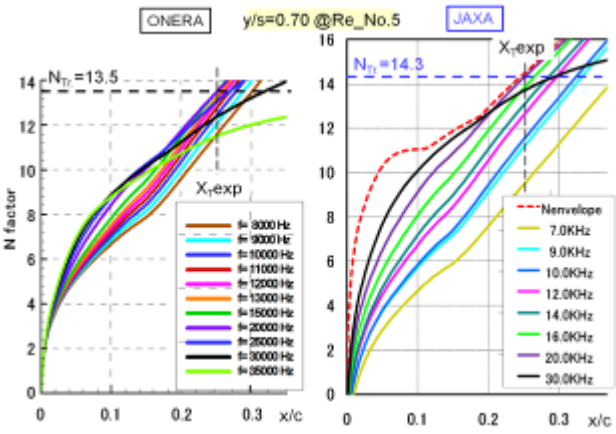

(b) y/s=0.7 (outer wing region)

Fig. 12. Stability characteristics with envelope strategy at Re_No.5

Fig. 13 shows similar comparison of N factors with fixed β strategy at Re_No.5. The range of several combinations of (β_r , f) was specified as follows:

$$-450 \le \beta_r[m^{-1}] \le 5000 \quad , \quad 3 \le f[kHz] \le 50$$

By comparing measured transition location with N factors at y/s=0.3 and 0.7, it was cleared that the most dominant instability mode was CFI at higher Reynolds number condition. Considering the whole spanwise stations reveals that the CFI mode is nearly dominant except for tip region (y/s=0.9) and kink region of leading edge (y/s=0.5) as shown in Fig. 14. N=12 provided by envelope strategy is in good agreement with measured transition data.

Against our expectation, CFI was not suppressed at such higher Reynolds number condition. It means present ideal pressure distribution for NLF wing is not optimum and should be improved. JAXA has already improved Cp_{Target} using JAXA's transition analysis code. Recently, JAXA has been conducting a new NLF wing design by using the improved Cp_{Target} and our CFD-based inverse design method.

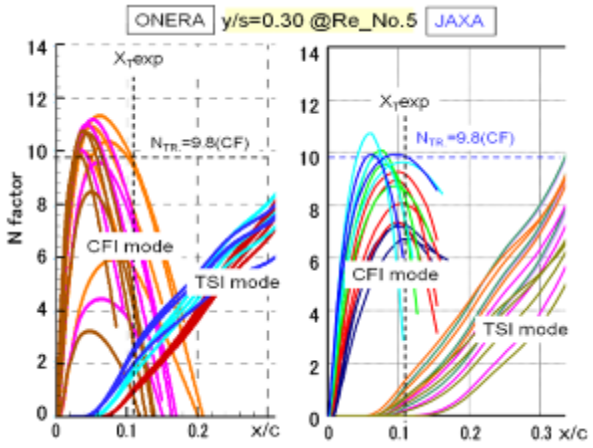

(a) y/s=0.3 (inner wing region)

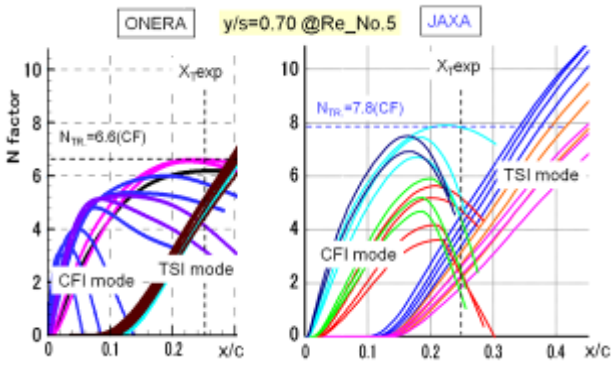

(b) y/s=0.7 (outer wing region)

Fig. 13. Stability characteristics with fixed β strategy at Re_No.5

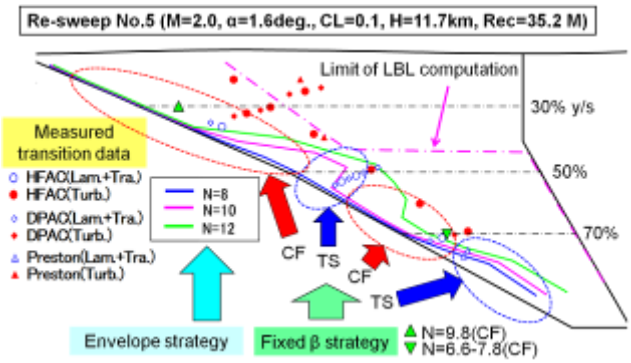

Fig. 14. Comparison of transition analysis and measurement results at higher Re No. point

4 Consideration Of Roughness And Reynolds Number Effects

4.1 Roughness Study

As mentioned above, surface quality has an important influence on transition process. As a matter of fact, CFI are very sensitive to surface roughness but any effective correction approaches on e^N method have not been established yet. Before and after the flight test, JAXA measured surface roughness height distributions using lots of sample pieces made of "resin" and laser displacement measurement system as shown in Fig. 15. Then, it was obtained that the NEXST-1 had averaged roughness height of about 1 μm as [Ra] metric.

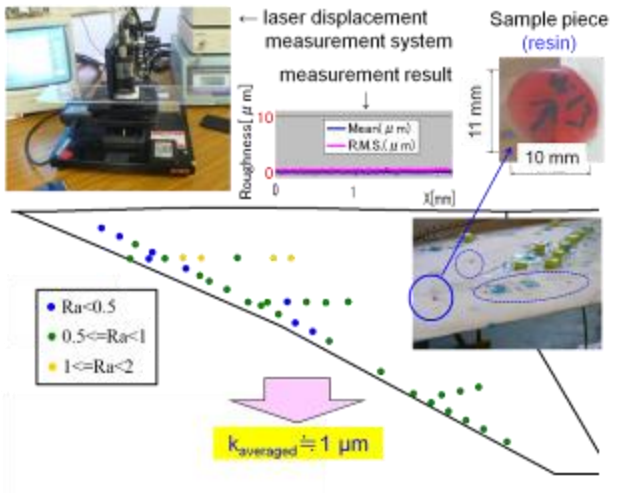

Fig. 15. Measured roughness height

Recently, ONERA obtained useful relation between Reynolds number based on roughness height (Rk) and transition N value in supersonic

flow condition [7] as summarized in Fig. 16. ONERA found out linear relation between Rk and N factor as illustrated in the figure, and JAXA approximated the linear relation with the following equation:

$$N = 16.25 - 6.61\log_{10} R_k \quad where \quad R_k \equiv \frac{u_k k}{\nu_k}$$

Then, JAXA computed Rk distributions of the NEXST-1 over whole wing surface at two flight test conditions (namely α_No.4 and Re_No.5), according to ONERA's approach for computing and plotting them. Fig. 17 shows computed Rk contour maps near leading edge at inner and outer wing region for the most severe case corresponding to the higher Reynolds number (case Re_No.5).

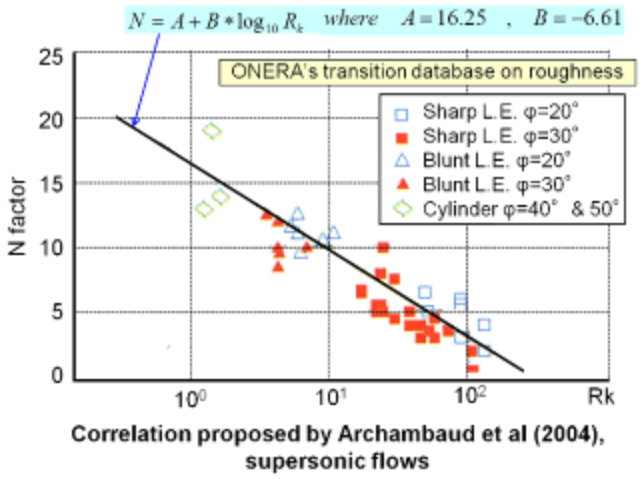

Fig. 16. ONERA's transition database on roughness [7]

As easily seen in the figure, the following result was obtained:

Rk＜0.05 (0.005<x/c<0.1)

This situation corresponds to N>24 in Fig. 16. Such an N value is too high to predict transition location due to influence of roughness. It means that such Rk value has little influence on transition phenomenon according to present ONERA's database. Naturally this consideration is also valid for transition phenomenon at α_No.4, because boundary layer thickness at the AOA case is larger than at case Re_No.5.

4.2 Reynolds Number Effect On NEXST-1 Flight Test

As mentioned above, JAXA's NLF wing design concept of the NEXST-1 was not effective at higher Reynolds number condition (Re_No.5). To understand this situation, Reynolds number effect on transition in three-dimensional laminar boundary layer is considered in this sub-section. First of all, whole experimental transition data are summarized in next part. In a second time, experimental transition locations are compared to the predicted numerical ones obtained with an assumed N factor critical value. Finally, the influence of Reynolds number on the nature of instability and transition process is investigated using the theoretical target pressure distribution.

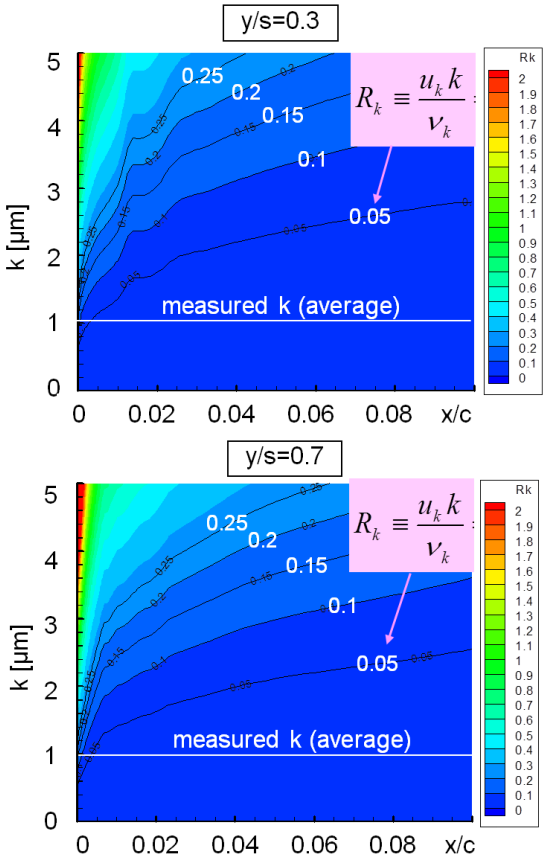

Fig. 17. Rk study at Re_No.5 condition

(1) Summary of experimental transition data

Fig. 18 shows the summary of transition measurement results of S2MA wind tunnel and NEXST-1 flight tests. The S2MA test results are described in Ref. [3] and stability analysis results with both envelope and fixed β strategies are summarized in Ref. [4] where influence of freestream turbulence and surface roughness on transition is also discussed.

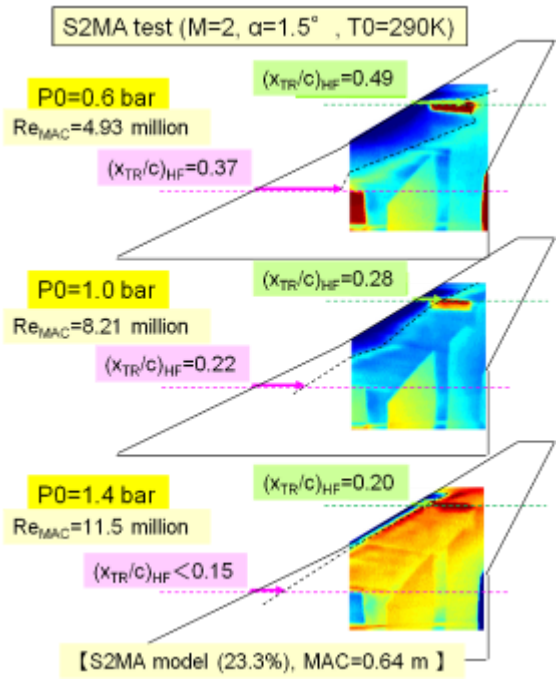

(a) S2MA test results [3]

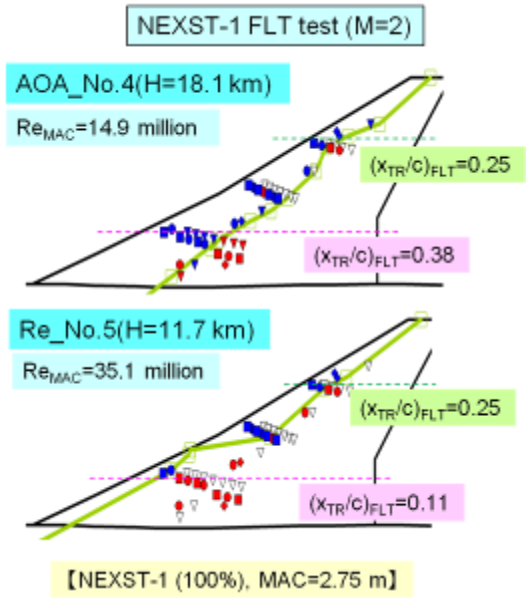

(b) NEXST-1 flight test results [5]

Fig. 18. Summary of Transition Measurement Results

Fig. 18(a) represents infra-red measurements in S2MA test section for three total pressures corresponding to chord Reynolds number range $4.93\times10^6<Re_{MAC}<11.5\times10^6$. Laminar zone corresponds to the darest area. From Fig. 18, behavior of transition location at outer wing region in the S2MA test case is different from that in the NEXST-1 flight test case when the Re_{MAC} increases. According to Rk study for the S2MA test model described in Ref. [4], influence of roughness was estimated to be little on transition, because measured roughness height of the model was about 1 μm, almost the same as the NEXST-1 meaning relatively small.

Therefore, it is supposed that the difference of the behavior of transition location originates in any influence of freestream turbulence and the difference of Cp contours of both models. It is not easy to analyze the influence of freestream turbulence by using present experimental data and current analysis methods. At next sub-section, the relation between Cp contours and transition is discussed.

(2) Comparison of measured and predicted transition locations

If it is assumed that transition is predicted with each constant N value over whole wing region at each freestream condition, $N \fallingdotseq 4.5$ for the S2MA test cases and N=12 for the NEXST-1 flight test cases are almost estimated as shown in Fig. 19. According to these values, Reynolds number based on chordwise transition location ($Re,x_{TR.}$) is predicted and compared with measurement results as shown in Fig. 20.

From Fig. 20(a), if the outer part of the wing, y/s=0.7 is considered, the evolution of transition Reynolds number in flight condition (indicated as "FLT") is different from the wind tunnel one. It implies that the measured transition location at y/s=0.7 in α_No.4 was too forward compared with the transition location predicted with the constant N value.

The fact of forward movement of measured transition at y/s=0.7 originates in the following subjects:

(a) Interpolated Cp contour did not completely coincide with measured Cp contour, especially spanwise variation of Cp distributions near y/s=0.7 is not well-interpolated.

(b) Measured Cp contour did not reflect the target Cp contour, especially near outer wing region.

As for the subject (a), additional stability analysis conducted with careful tuning some parameters on our surface-interpolation technique near the region at y/s=0.7 indicates

that correlation between measured and predicted transition locations was slightly improved, but not fully. JAXA has not cleared this point yet.

As for the subject (b), further stability analysis on the Cp_{Target} contour was performed as described in next sub-section.

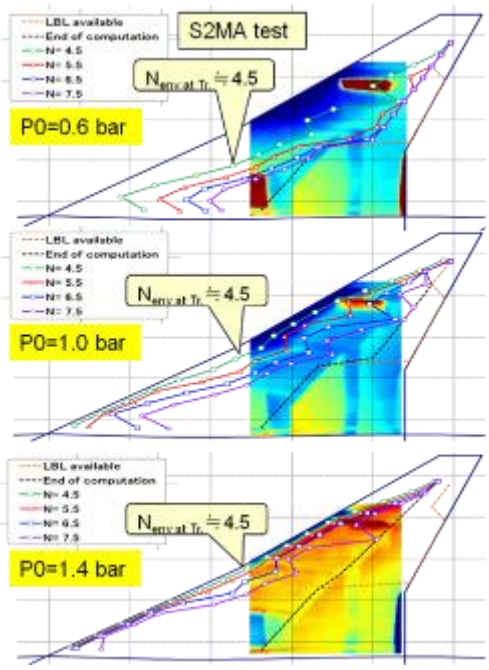

(a) S2MA test results

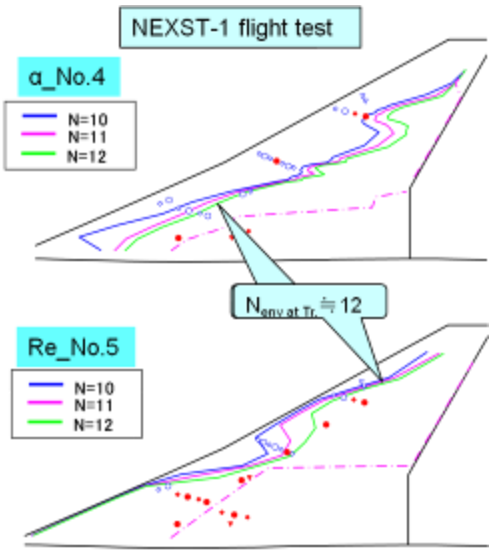

(b) NEXST-1 flight test results

Fig.19. Comparison of estimated transition N (envelope strategy) and experiments

(3) Reynolds number effect on the target Cp contour

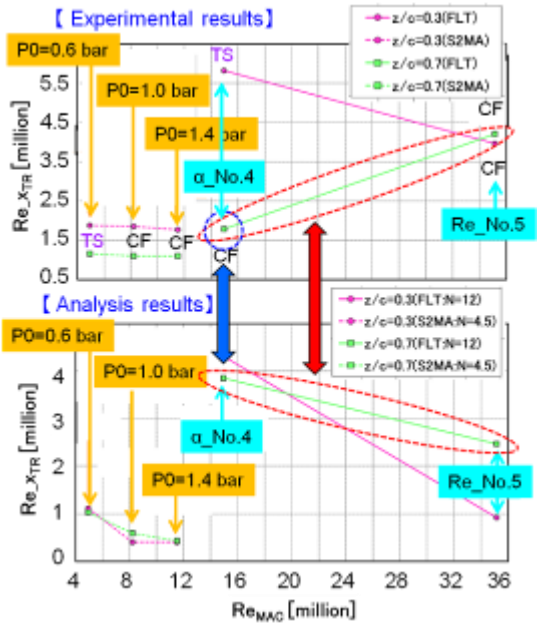

Fig. 20. Chord Reynolds number effect

At first, comparison of the Cp_{Target} and present surface-interpolated Cp contours is shown in Fig. 21. As easily seen, there is remarkable difference at outer wing region. This originated in non-completion of convergence at the NEXST-1 NLF wing design [2]. Stability analysis results on both Cp contours are summarized in Fig. 22. It indicates the Cp_{Target} contour has possibility to delay the transition at outer wing region more strongly than at the experimental interpolated one.

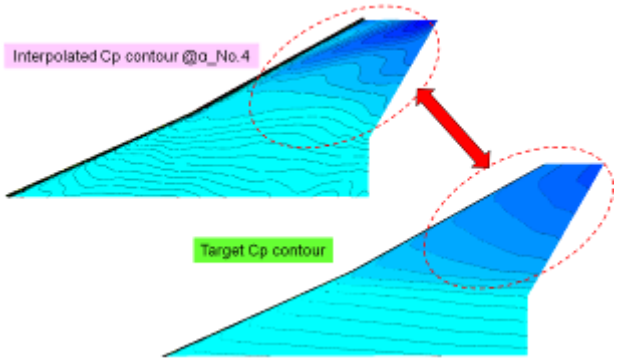

Fig. 21. Comparison of Target and interpolated Cp contours at design point

Reynolds number influence on transition process (nature of instability and transition location), has been numerically investigated using the theoretical target pressure distribution. N factor values provided by fixed β strategy at

the mid span region (y/s=0.5) are plotted in Fig.23 as a function of the dimensionless streamwise station for two typical chord Reynolds numbers. To understand physical nature of transition, namely identify the most dominant instability, fixed β strategy computations have been undertaken.

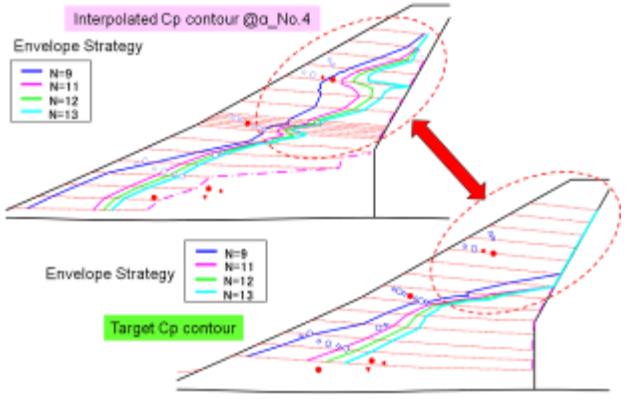

Fig. 22. Comparison of N contours on target and interpolated Cp contours at design point

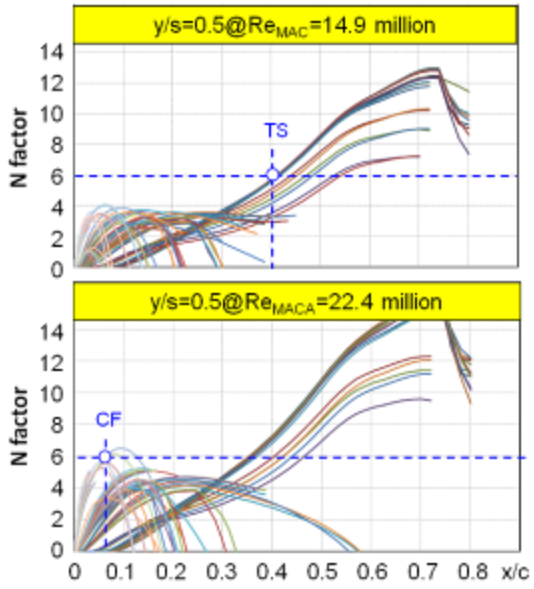

Fig. 23. Reynolds number effect of N factors on Target Cp distributions

To consider Reynolds number effect clearly, if 6 is assumed as a critical transition N factor value, the dominant mode is TSI for the lower Reynolds number case. Up to the higher Reynolds number case, transition is triggered by CFI. As a matter of fact, as chord Reynolds number Re_{MAC} increases, amplification of crossflow instabilities in the leading edge region is enhanced. The evolution of dimensionless transition location, corresponding to $N_{TR.}$=6, as a function of chord Reynolds number, for y/s=0.5, is plotted in Fig. 24 (green line). Open symbols stand for TSI driven transition whereas full symbols represent CFI induced transition. Up to $Re_{MAC}<22.4\times10^6$, transition is triggered by TSI and its position slightly moves upstream when Re_{MAC} increases. $Re_{MAC}=22.4\times10^6$, as represented in Fig. 23, CFI are sufficiently amplified to reach the critical transition N value: therefore, the transition dramatically moves towards the leading edge and will take place all the more close to the leading edge than the Reynolds number is high.

This physical change of transition phenomenon is illustrated by the drop of the green line represented $(x/c)_{TR}$. as a function of chord Reynolds number at $Re_{MAC}\approx22.4\times10^6$ in Fig. 24. Same kind of analysis has been carried out for y/s=0.3 and 0.7. All the results are gathered in Fig. 24. For the inner part of the wing, y/s=0.3, transition is induced by CFI even for low Reynolds number. For the outer part of the wing, y/s=0.7, the evolution is very similar to the one obtained at y/s=0.5.

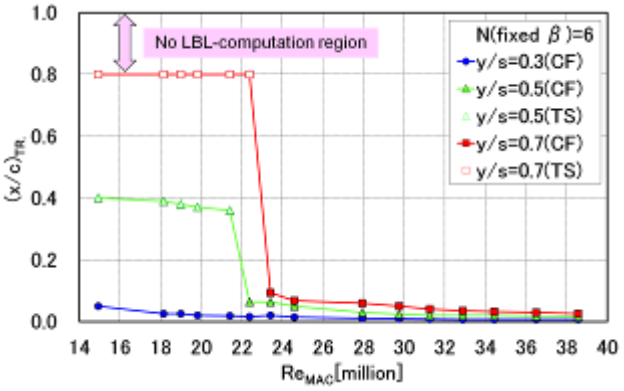

Fig. 24. Re No. effect on transition location of target Cp distribution predicted with N=6 based on fixed β strategy

As mentioned before, the predicted transition rapidly moves near the leading edge region, around $Re_{MAC}\approx22.4\times10^6$, because of the change of instability nature from TSI to CFI. Therefore, JAXA's NLF wing design concept completely based on the Cp_{Target} contour has possibility of large laminarity at outer wing region at $Re_{MAC}<22.4\times10^6$ under the

approximation of selecting N=6 as a transition criterion.

5 Concluding Remarks

Principal results in present research are as follows;
(a) Stability analysis with envelope strategy shows good correlation between measured transition location and N contour, for example $N_{TR.}$=12 for NEXST-1 flight test and 4.5 for S2MA wind tunnel test conditions.
(b) Stability analysis with fixed β strategy makes clear dominant instability mode at measured transition location. Both parties confirmed well-suppression of CFI on the NEXST-1 at the design point in flight test and at lower Reynolds number case in S2MA wind tunnel test.
(c) Investigation of chord Reynolds number (Re_{MAC}) effect on transition characteristics on experimental results shows similar feature on predicted transition results for variation of Re_{MAC}, except for outer wing region (y/s=0.7) in flight test case. This exception is thought to be induced by non-completeness of realizing the Cp_{Target} at the design point in flight test.
(d) According to roughness study with measured roughness height of about 1 μm on NEXST-1 and S2MA test model, there is no influence on transition location based on ONERA's experimental database.
(e) It was obtained that the Cp_{Target} for NEXST-1 design has great potential to delay transition location at the design point. Nonetheless, transition moves rapidly from mid-chord position (TSI-dominant) to forward position (CFI-dominant) as Re_{MAC} increases above 22.4 millions.

Finally, as conclusion of present joint research in about 10 years, ONERA and JAXA obtained valuable knowledge of transition in supersonic flow, for example, cross-validated e^N methods, NLF wing effect (well-suppressed CFI), useful relations (as database) on roughness, freestream turbulence and Reynolds number effects.

Acknowledgement

The authors would like to express special thanks to Dr. Olivier Vermeersh of ONERA for stability analysis of S2MA test and roughness study. Furthermore, the authors also would like to thank Mr. Hiroaki Ishikawa of JAXA for CFD computations of several flow conditions.

References

[1] Yoshida K, Sugiura H, Ueda Y, Ishikawa H, Tokugawa N, Atobe T, Takagi S, Arnal D, Archambaud J.P, Seraudie A. Experimental and Numerical Research on Boundary Layer Transition Analysis at Supersonic Speed: JAXA-ONERA cooperative research project. JAXA-RR-08-007E, March, 2009

[2] Yoshida K. Supersonic drag reduction technology in the scaled supersonic experimental airplane project by JAXA. Progress in Aerospace Sciences, vol.45, pp.124-146, 2009

[3] Sugiura H. Yoshida K, Tokugawa N, Takagi S. and Nishizawa A. Transition measurements on the natural laminar flow wing at Mach 2. Journal of Aircraft, vol.39, No.6, pp.996-1002, 2002.

[4] Vermeersh O, Yoshida K, Ueda Y, Arnal D. Transition Prediction on A Supersonic Natural Laminar Flow Wing: Experiments and Computations. 47th International Symposium of Applied Aerodynamics, Paris, 26-28 march 2012.

[5] Yoshida K, Kwak D.Y, Tokugawa N, Ishikawa H. Concluding Report of Flight Test Data Analysis On The Supersonic Experimental Airplane Of NEXST Program By JAXA. ICAS2010-2.8.2, 2010

[6] Arnal D. Boundary layer transition: predictions based on linear theory. AGARD FDP/VKI Special Course on "Progress in Transition Modeling", AGARD Reprt 793, 1993.

[7] Arnal D, Casalis G and Houdeville R. Chapter 7-Practical Transition Prediction Methods: Subsonic and Transonic Flows. ONERA Report, RF 1/13639 DMAE – September 2008.

Copyright Statement